



EMULSION FLOW MODEL BASED ON MOBILITY CONTROL AND DISPLACEMENT EFFICIENCY EFFECTS

Ranena V. Ponce Flores

Márcio S. Carvalho

PUC-Rio, Department of Mechanical Engineering, R. Marquês de São Vicente 225, Gávea, 22453-900, Rio de Janeiro, RJ - Brazil
poncerv@puc-rio.br, msc@puc-rio.br

Vladimir Alvarado

University of Wyoming, Department of Chemical and Petroleum Engineering, Laramie, WY 82071, U.S.A.
valvarad@uwyo.edu

Abstract. *Emulsion flooding has a significant potential as an enhanced-oil recovery (EOR) strategy. Additionally, recovery mechanisms of several chemical EOR methods, including alkaline and alkaline-surfactant flooding applied to heavy oil, are consistent with the formation of in-situ emulsions. To enable emulsion flooding designs, EOR recovery mechanisms must be adequately represented in reservoir simulators to upscale pore-level effects to the continuum in porous media. In this work, we have incorporated two known effects of emulsion flooding, namely an increased pore-level displacement efficiency and second, a macroscopic mobility control, through a parametrization of the relative permeability curves as functions of the dispersed phase concentration. In the first mechanism, relative permeability end-point saturation was parameterized with respect to the dispersed phase concentration to allow mobilization of residual oil after waterflooding. The second mechanism was modeled through changes of the end-point value of the water relative permeability. Experimental results of water and emulsion flooding of viscous oil were history-matched. A parametric analysis of a 1/4 of a 5-spot geometry shows that the main contribution to incremental oil recovery observed experimentally corresponds to increase in the displacement efficiency. However, if viscous fingering is allowed to occur, a benefit of mobility control is observed in the case of more unfavorable mobility ratio. Attention must be paid to details of the relative permeability curves and not only to oil viscosity. The results indicate that properly designed emulsions should produce significant recovery benefits.*

Keywords: *Emulsions, Dispersed flow, Porous media, Mobility control, Enhanced oil recovery.*

1. INTRODUCTION

Flow of complex fluids in pore-level geometries shows responses that can not be explained based on bulk rheological properties. This is the case of polymer solutions, which exhibit non-Newtonian rheological behavior such as shear-thickening or shear thinning effects (Sorbie, 1991; Kazempour *et al.*, 2012), and emulsion solutions, which macroscopic performance depends on several parameters as the pore-throat radii to the dispersed phase drop size (Cobos *et al.*, 2009). Beyond differences observed in the flow response outside and inside porous media, fluid-fluid interactions also affect most of the oil recovery technologies used to increase oil production efficiency. A common problem in the oil industry, mostly during waterflooding, is the presence of an adverse mobility ratio between the displacing and displaced fluids. Under such condition, interfacial viscous instabilities occurs in the injection front (Homsy, 1987) causing early water breakthrough by creating a preferential flow path to the producing wells and consequently low sweep efficiency.

Emulsions can be used to overcome this downside by using them as mobility control agents. The emulsion mechanism is based on capillary resistance (Jamin effect) and characterized experimentally by two singular effects observed in what we denote as Water-Alternating-Emulsion (WAE) flooding. The first of them is the movement of residual oil left behind water injection (Guillen *et al.*, 2012a). This improvement in pore-level displacement efficiency can be described by using the concept of ganglia dynamic (Payatakes, 1982). When the previous waterflooded pore space is blocked by the emulsion dispersed phase, water flow diverts to reservoir unsweep areas mobilizing trapped oil by overcoming capillary pressure differences through viscous pressure gradient all along the oil ganglia. The second effect is the reduction of the water mobility. An increased volumetric sweep efficiency results from this mechanism since the pore blockage stabilizes the injection front plugging water channels and inhibiting further fingering development.

Oil-in-water (O/W) emulsion injection used as EOR method has shown demonstrable sweep efficiency improvement from its first tests in the 1970's (McAuliffe, 1973a). More over this effect were also evidenced by recovery of extra oil during the flooding of heavy oil emulsions formed *in-situ* by reduction of water mobility (Jennings *et al.*, 1974). The later results was confirmed by Zhang *et al.* (2010) who found that mobility reduction overcomes low interfacial tension effects as dominant enhanced recovery mechanism by a well correlation among pressure drop and recovery enhancement. However, since fluid flow at pore-level is governed by competition between capillary and viscous forces, the local velocity

of the bulk fluid carrying the dispersed phase has a relevant impact on the emulsion performance to improve oil recovery. In fact, studies of capillary effects during emulsion flooding in sandpack and sandstones made by Dong *et al.* (2009) and Guillen *et al.* (2012b) revealed that oil recovery decreases at high flow rate. This flow behavior of emulsions was reproduced at mesoscale by Romero *et al.* (2011) who develop a capillary network model that uses experimental pore-level constitutive relationships of the flow through constricted quartz microcapillaries. Experimental flow response of emulsion injection in sandstones showed a qualitatively match with numerical results and the expected mobility-capillary number dependence, confirming the underlying mechanism of emulsion flooding.

Macroscopic modeling of such complex flow is essential to develop feasibility analysis of emulsion injection as EOR method. However formulation of accurate models is challenging because this require not only a thorough knowledge of the involved multiphase phenomena but to describe properly the key parameters so their contribution matched reasonably the observed results at the macroscale.

In this work, we present a reservoir modeling strategy of emulsion flooding by incorporating relative permeability curves that depend on the emulsion dispersed phase concentration. The two main experimental effects observed after emulsion injection, enhancement in oil sweep efficiency and water mobility control, were embedded in the oil-emulsion relative permeability curves. This strategy was used to history-match corefloods experiments of emulsion displacing heavy oil on sandstone samples and to create synthetic curves for emulsion displacement with medium and light oils. We implemented a 2D heterogeneous model at lab scale using a pseudo-compositional commercial reservoir simulator (CMG-STARSTM) containing one injection well and one producer in a one-quarter of a 5-spot arrangement. A parametric analysis on WAE flow was carried out to determine the impact in oil recovery of the emulsion Kr-curves, fluid viscosity, mobility ratio as well as operational parameters.

2. EMULSION SIMULATION MODEL

Experimental results (McAuliffe, 1973a,b; Cobos *et al.*, 2009; Romero *et al.*, 2011) suggest that Jamin effect can be responsible for water mobility reduction in pores blocked by emulsion drops large enough to get trapped by capillarity. This change in the mobility of the emulsion continuous phase can be described in continuum models through reduction of its relative permeability, behavior that has been observed experimentally (Arhuoma *et al.*, 2009b; Engelke *et al.*, 2013).

Arhuoma *et al.* (2009b) modeled alkaline flooding of heavy oil based on the *in situ* formation of water in oil (W/O) emulsions. In the model two aqueous phases (water and alkaline solution) and two oil components (crude oil and W/O emulsion) are considered and a pseudo-reaction used to get *in situ* formation of W/O emulsion during alkaline flooding. Since they modeled W/O emulsions, it was used a correlation of viscosity with respect to emulsion concentration (Arhuoma *et al.*, 2009a) as well as changes in IFT and chemical adsorption to properly model alkali flooding. Experimental relative permeability curves were determined by using the JBN method (Johnson *et al.*, 1959) which is a semi-analytical unsteady-state determination that neglects capillary pressure. Experimental water relative permeability results in alkaline flooding confirmed lower Kr values at the same water saturation compared to that of waterflooding. To locally incorporate the mobility performance effects in the model, Arhuoma *et al.* (2009b) interpolate between water and emulsion flooding relative permeability curves. They found a good match for recovery and pressure drop, being the main explanation for recovery the increase in sweep efficiency.

In the present work, we study the injection of a stable O/W macro emulsion. Romero *et al.* (2011) reported that these emulsions behave as Newtonian fluids in the range of shear rate of interest and typical of EOR flooding. In our model, we consider two fully miscible aqueous phases (water and emulsion) and one oil component in the oleic phase that saturates the porous media. In the model, each emulsion slug injection was handled by stabilizing a non-zero molar fraction of the emulsion phase. We assume the viscosity and density of the emulsions very similar to that of water since the dispersed-phase concentration is not high ($\leq 10\%$). The emulsion's improved pore-level displacement efficiency and macroscopic mobility control were embedded on the relative permeability curves, allowing interpolation among oil-water and oil-emulsion relative permeability curves as function of the dispersed phase concentration during emulsion flooding. For the sake of simplicity we assumed that the local capillary number is low enough so that blockage of pores of throat sizes smaller than emulsions drops size remains essentially constant (Romero *et al.*, 2011). A more complete model should include the drop's straining and capture dependence as a function of capillary number, but this approach is beyond of the scope of this work.

3. RESULTS AND DISCUSSION

To investigate the effectiveness of the emulsion flow during WAE processes on different oils, we analyzed three cases of oil-water viscosity ratio, each one with its corresponding set of relative permeability curves. Case I defines the highest viscosity ratio scenario with $\mu_o/\mu_w = 427$. In this case, relative permeability curves were calculated for a heavy-oil through history-matching coreflooding production data published by Guillen *et al.* (2012b). Case II corresponds to a viscosity ratio $\mu_o/\mu_w = 100$. In this case, we used oil-water and oil-emulsion relative permeability curves obtained by Engelke *et al.* (2013) through steady-state flow experiments. Case III represents a light oil case with a viscosity ratio

of $\mu_o/\mu_w=10$. Since experimental data were not readily available, we used Corey's model (Corey, 1954) to generate synthetic curves similar to published relative permeability sets for light-oil in a weakly water-wet media. The three cases were run on one-quarter of a 5-spot well pattern represented through one layer of $100 \times 100 \text{ m}^2$ discretized in $50 \times 50 \times 1$ cells. In the model was assigned a homogeneous porosity of 0.273 and a heterogeneous permeability field, depicted in Figure 1, was obtained using a Dykstra-Parsons (Dykstra and Parsons, 1950) variation coefficient of $DPV=0.7$ for an average absolute permeability of 124.36 mD.

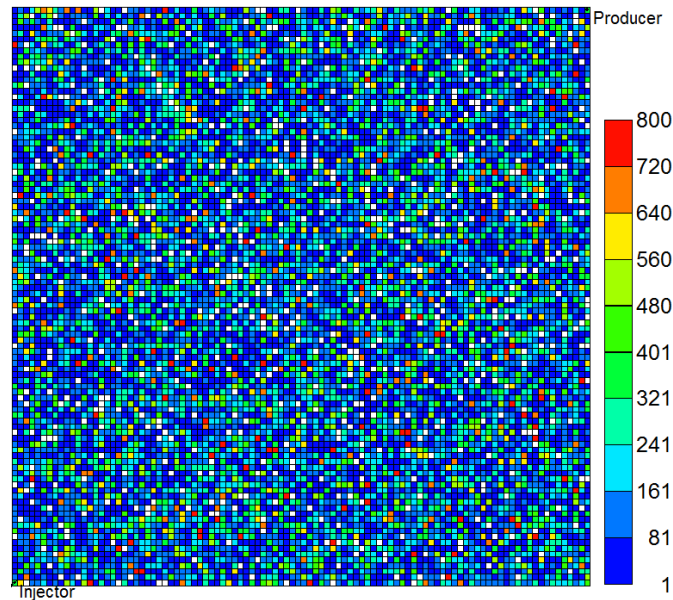


Figure 1. Absolute permeability map used in the simulations obtained with $DPV=0.7$ for $\bar{K}=124.36 \text{ mD}$.

In the simulations, the injection flow rate was set at $Q = 8.33 \times 10^{-6} \text{ m}^3/\text{s}$ and waterflooding carried on for a number of pore volumes (PV) followed by the injection of a 1 PV emulsion slug, ultimately chased by continuous water injection. The time for the emulsion slug injection was varied to determine its impact on production behavior. The fully implicit solver of CMG STARS 2011.102G was used to simulate the oil displacement by WAE injection, using the proposed model.

3.1 Case I. Relative permeability curves from history-matched transient flow

We history-matched the low-capillary number experimental results obtained by Guillen *et al.* (2012b) to generate the oil-water and oil-emulsion set of relative permeability curves. In the experiments, the porous medium consisted of a sandstone core of length $L=0.06 \text{ m}$, diameter $D=0.038 \text{ m}$, porosity $\phi=0.253$, and absolute permeability $K=262 \text{ mD}$. The properties of the oil used in these experiments (Shell Talpa 30) were $\mu_o=0.427 \text{ Pa}\cdot\text{s}$ and $\rho_o=908 \text{ Kg/m}^3$. The water viscosity and density were $\mu_w=0.001 \text{ Pa}\cdot\text{s}$ and $\rho_w=1000 \text{ Kg/m}^3$, respectively. To history match experimental data, a cartesian grid with $42 \times 1 \times 20$ cells and grid size of $(0.16 \times 3.33 \times 0.17) \times 10^{-6} \text{ m}^3$ was set up. Two additional columns of gridcells with $K=5000 \text{ mD}$ were added at both ends of the domain to place injection and production wells in order to simulate the boundary conditions. The experimental injection rate of $5 \times 10^{-10} \text{ m}^3/\text{s}$ was set as a constraint for the injector, while the producer was controlled by setting the bottomhole at atmospheric pressure. A Corey-type relative permeability model was used in the simulation. Since capillary pressure data was unavailable, we disregarded this effect.

Figure 2 presents the experimental data together with the fitted production curve. In the experiment, initial waterflooding were conducted for more than 13 PV to guarantee residual oil saturation. This data set was used to determine the oil-water relative permeabilities. At this point, a slug of 1.1 PV of emulsion was injected to match experimental data, followed by a second waterflooding. This data set was used to obtain the oil-emulsion relative permeabilities.

Figure 3 shows the oil-water and oil-emulsion relative permeability curves resulting from history-matching. These curves are similar in trend to results of relative permeability curves found by Engelke *et al.* (2013) from production data collected during steady-state experiments of oil-emulsion displacements, and also by Arhuoma *et al.* (2009b) through history matching of alkali-surfactant flooding with in-situ emulsion formation. The main characteristics of relative permeability curves during emulsion flooding is the reduction of the residual oil saturation, behavior that combines both effects, an improve on pore-level displacement and macroscopic sweep efficiency. The history matching yielded an irreducible water saturation of $S_{wi}=0.12$ as in the experiments, while the residual oil saturation that best matched experimental data was for oil-water $S_{orw}=0.58$ and $S_{ore}=0.45$ for oil-emulsion. The Corey exponents was $n_o=0.8$ and for both aqueous phases $n_w=4$.

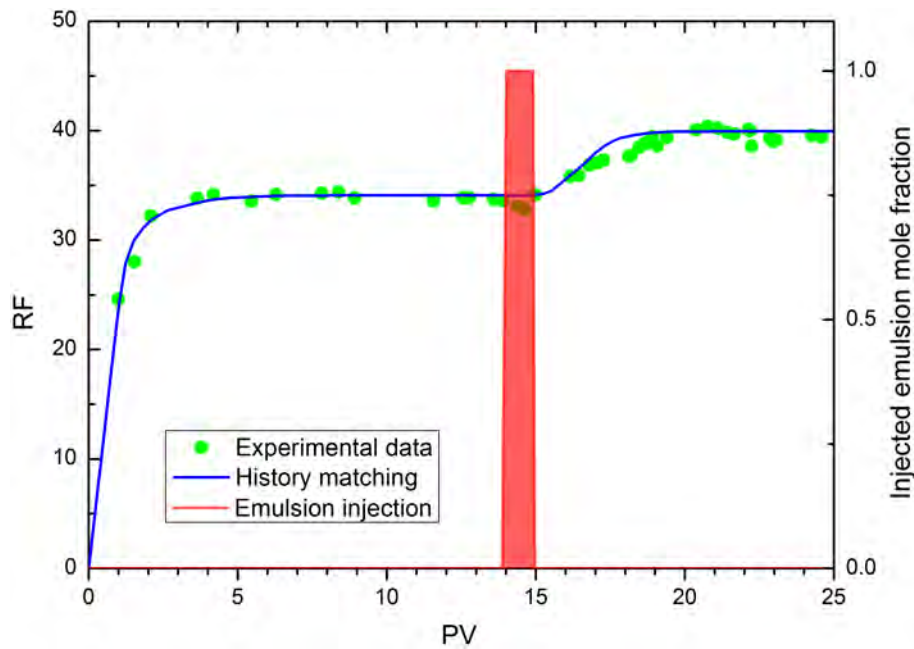


Figure 2. Experimental data of (Guillen *et al.*, 2012b) and production curve obtained by history-matching.

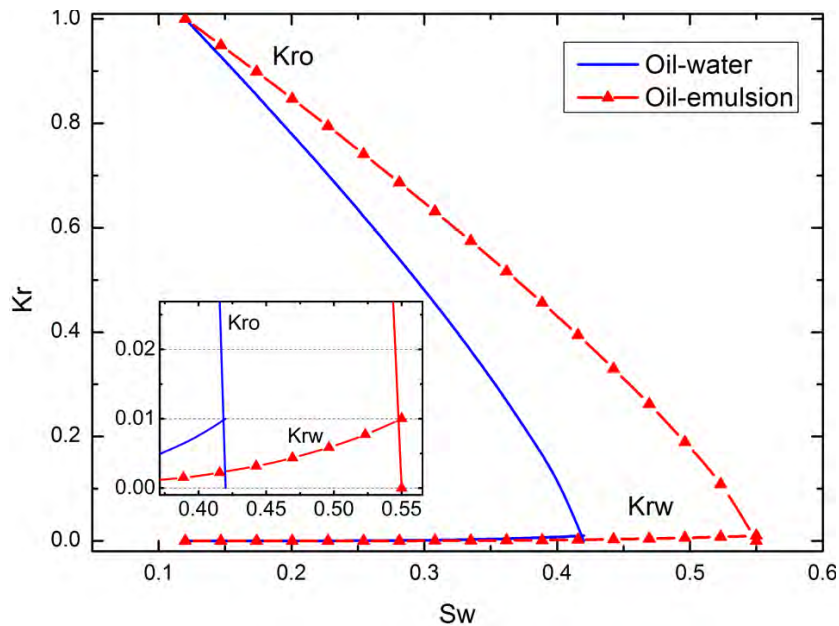


Figure 3. Relative permeability curves resulting from history-matching water and emulsion flooding production results of (Guillen *et al.*, 2012b)

It is interesting to notice that despite the high oil viscosity, the mobility ratio M , defined in Equation (1), turned out to be the lowest among the three cases, at $M \approx 4$.

$$M = \frac{k_{rw} (1 - S_{or}) / \mu_w}{k_{ro} (S_{wi}) / \mu_o} \quad (1)$$

In order to investigate the effect of mobility control alone, synthetic oil-emulsion relative permeability curves were created. To ensure no effect in S_{ore} , the oil relative permeability was kept the same as in the waterflooding case, while the water relative permeability was generated by rescaling the end-point of the water curve for a more favorable mobility ratio of $M=2$. The resulting curves are depicted in Fig. 4.

Figure 5 shows the oil recovery factor (RF) for waterflooding and both WAE injection. In the simulation the emulsion slug was injected after 2.8 PV of waterflooding to reach a watercut greater than 99%. A significant increase in oil recovery is observed with the history-matched oil-emulsion curves, despite the fact that the emulsion was injected at near 100% watercut. On the other hand, the predictions obtained with the synthetic oil-emulsion curves, that only accounts for

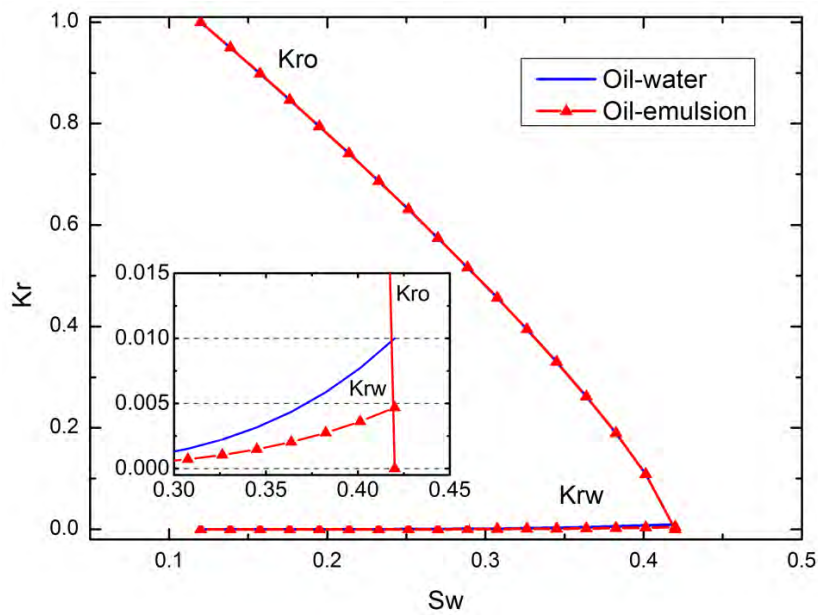


Figure 4. Synthetic relative permeability curves built from the history-matched curves to represent a pure mobility control mechanism.

mobility control effect, shows an insignificant increment in oil recovery, barely noticeable in Figure 5, despite having a 2-fold drop in water mobility. To analyze this, in Fig. 6 we show the water saturation maps generated at times labeled in Fig. 5 for water breakthrough (a), and for the emulsion stages (b),(c),(d) and (e) corresponding to the beginning, progress, breakthrough and end of the emulsion injection respectively.

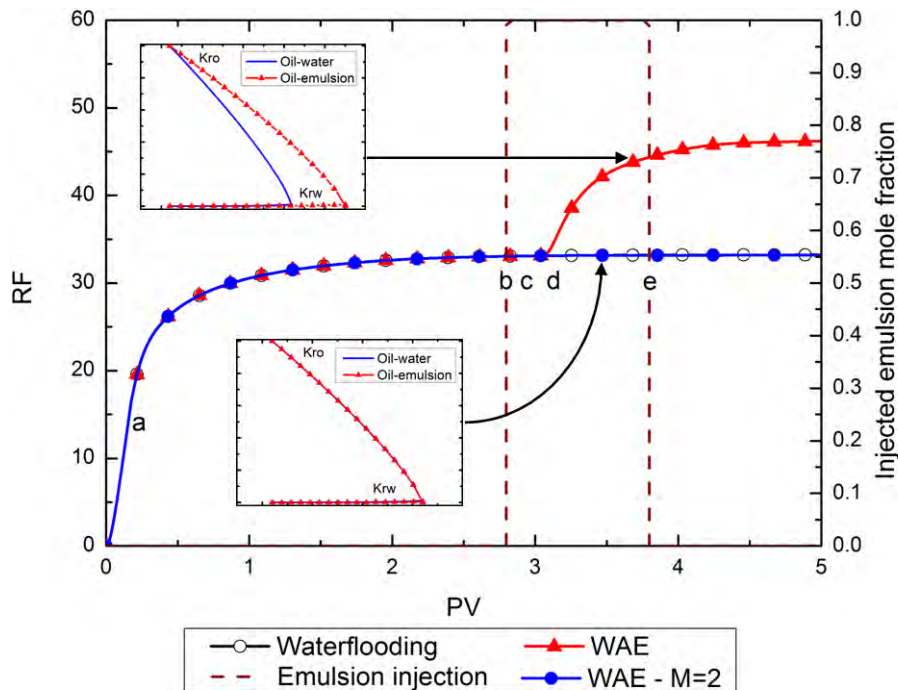


Figure 5. RF for waterflooding and WAE injection using both sets of Kr-curves presented in Figs.3 and 4. Emulsion slug was injected at 2.8 PV.

In Figure 6 the upper three water saturation frames correspond to the history-matched permeability curves and the lower frames to the results of mobility control alone. It is apparent in frame (b) that when the emulsion injection begins the reservoir area containing mobile oil was small, which explains the insignificant additional recovery from mobility control alone. The particular shape of the relative permeability curves for Case I leaves little room to take advantage of the mobility control effects after a long waterflooding period, as waterflooding is efficient in this case. During the

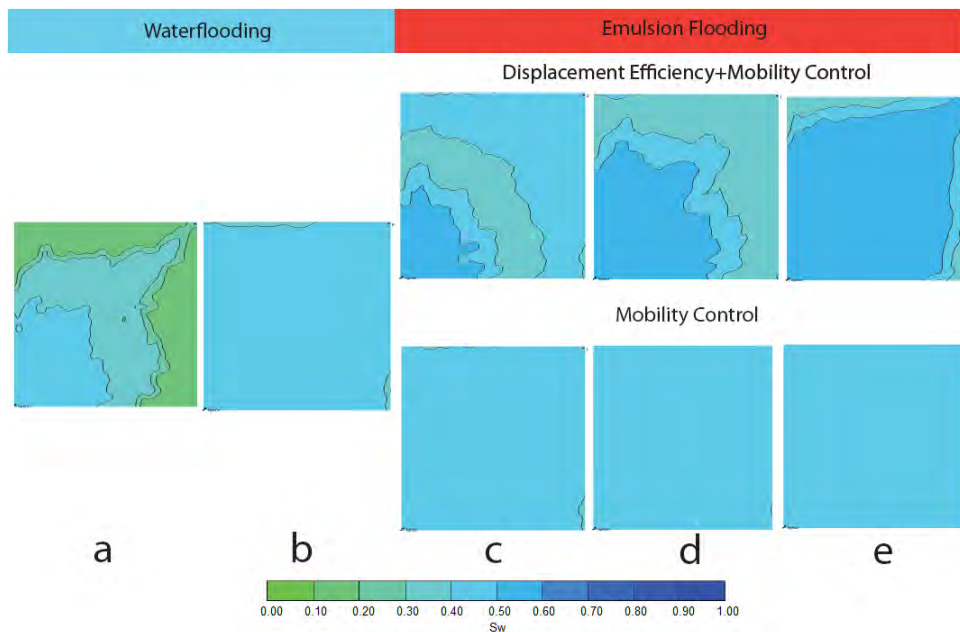


Figure 6. Water saturation maps for WAE injection using history-matched relative permeability curves (top) and synthetic mobility control curves (bottom).

emulsion injection in the upper frame (c), the improved pore-level displacement efficiency, characterized by a lower residual oil saturation in the history-matched curves, contributes to the formation of an oil bank, which is driven toward the production well. The obvious conclusion is that at least for the operating conditions analyzed, mobility control alone will offer little benefit from emulsion flooding. However, mobility control may accelerate oil production if the emulsion slug is injected earlier in the process, before water breakthrough. To prove this, we run the model with pure mobility control effect injecting the emulsion slug after 0.1 PV of water. Results of cumulative oil production and oil volumetric flow rate for WAE injection and waterflooding are depicted in Figure 7.

Although WAE injection show a weak effect, a more sustained oil rate under WAE injection leads to production acceleration noticed by a slightly higher cumulative oil response. On the other hand, the long-term cumulative oil production is the same. However, if we consider that waterflooding processes carried on for more than 1 PV are accompanied by high water cuts, the benefit of early emulsion flooding is not negligible.

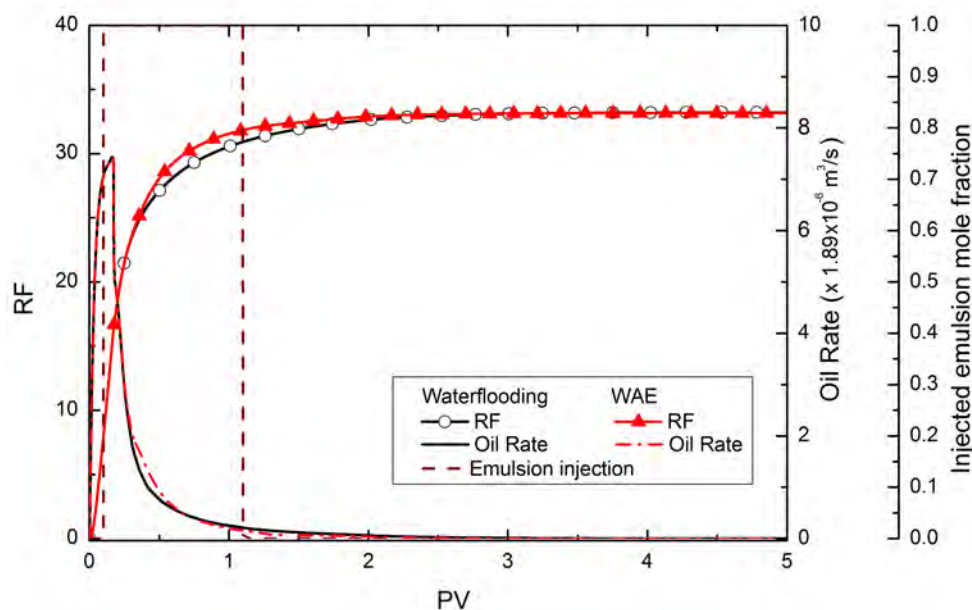


Figure 7. RF for waterflooding and WAE injection using the mobility control mechanism permeability curves presented in Fig.4. Emulsion slug was injected at 0.1 PV.

3.2 Case II. Relative permeability curves from steady-state flow

In this case, we used the oil-water and oil-emulsion relative permeability curves shown in Fig.8(a) measured by Engelke *et al.* (2013) from steady-state two-phase flow experiments. From the curves it can be noticed that the residual oil saturation were lowered from $S_{orw}=0.65$ for oil-water to $S_{ore}=0.45$ for oil-emulsion. Although the oil and water viscosity values in the experiments were 0.1042 Pa.s and 6.4×10^{-4} Pa.s (44°C) respectively, the mobility ratio were $M \approx 15$, the most unfavorable of the three cases analyzed. Similarly to Case I, we constructed a synthetic set of oil-emulsion relative permeability curves to studied the effect of mobility control alone for a more favorable mobility ratio ($M=2$). This curves are presented in Fig.8(b).

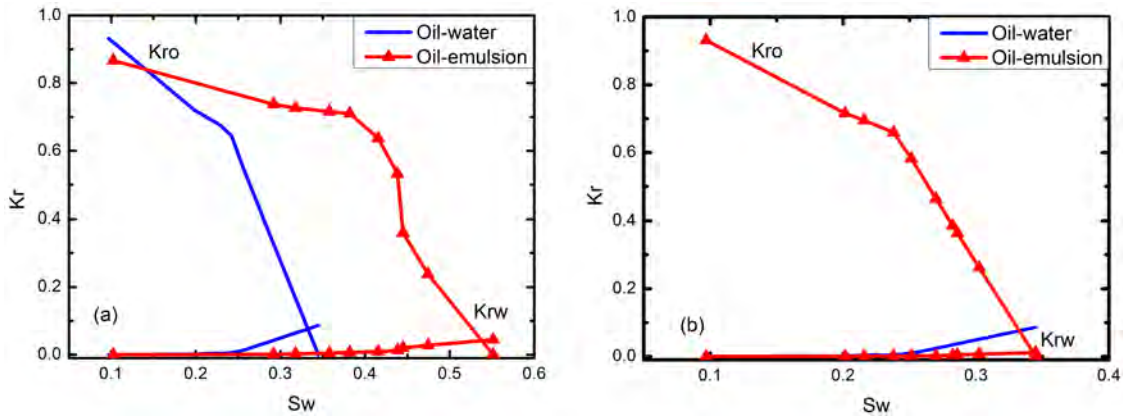


Figure 8. Relative permeability curves used in Case II: (a) obtained experimentally by Engelke *et al.* (2013); (b) Synthetic curves built from the previous set to analyze a pure mobility control mechanism.

Oil recovery for water injection and both WAE processes are shown in Figure 9. Results show a significant gain in oil recovery when using the experimentally determined relative permeability curves while the predictions using the curves with mobility control alone revealed an observable, but negligible effect.

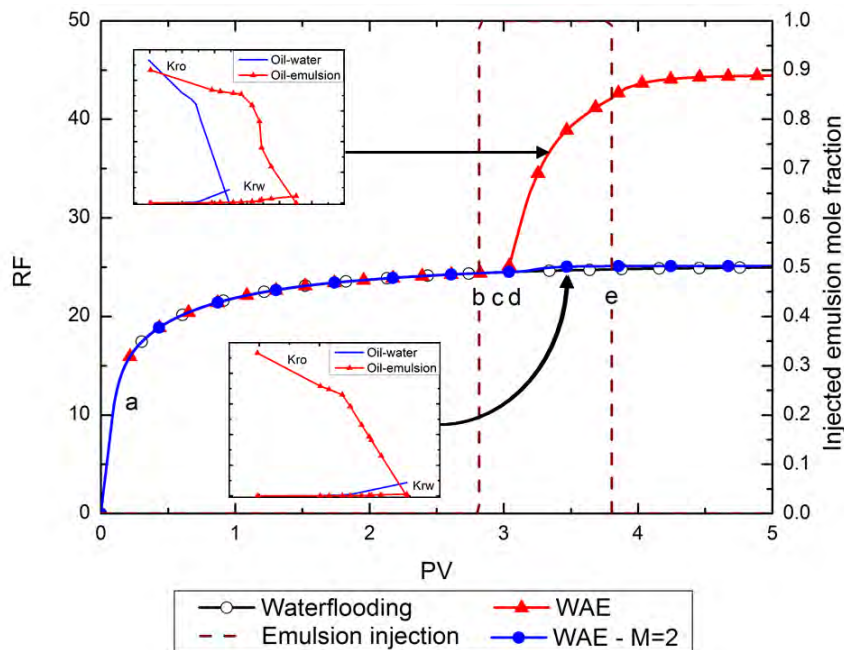


Figure 9. RF for waterflooding and WAE injection using both set of curves presented in Fig. 8. Emulsion slug was injected at 2.8 PV.

To analyze the production results, water saturation maps during flooding at the times highlighted in Fig. 9 were displayed in Fig.10. In frame (a), at the water breakthrough, it can be seen a more acute fingering when comparing with the predictions of Case I. Frame (b) shows a poor aerial sweep due to the worse mobility ratio, leaving considerable mobile oil behind the waterflooding front. After emulsion injection in the upper frame (c), it is possible to see an oil bank generated ahead of the emulsion front. As in Case I, the more uniform sweep effect led by pure mobility control

can be strongly affected by early water production. The small but noticeable incremental recovery suggest that emulsion injection before water breakthrough could yield benefits even in the pure-mobility control case.

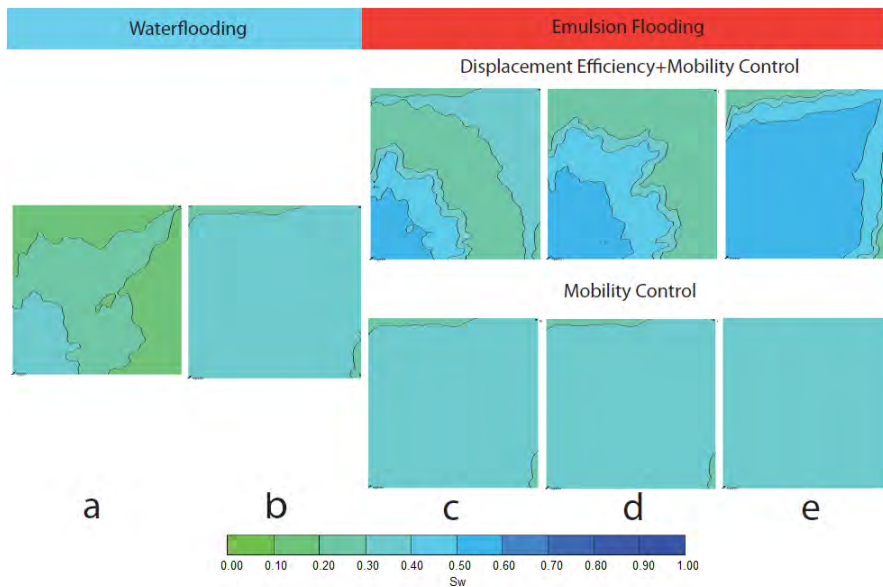


Figure 10. Water saturation maps for WAE injection using the relative permeability curves obtained by Engelke *et al.* (2013) (top) and synthetic mobility control curves (bottom).

Figure 11 shows cumulative oil production as well as oil volumetric flow rate for waterflooding and WAE injection (mobility control alone), being this time the slug of emulsion injected after waterflooding by 0.1 PV. As expected, production acceleration is more significant when compared to Case I and late emulsion injection in Case II. In the graph, formation of a small oil bank can be recognized by the small peak in oil rate, this evidences that fingering was arrested somewhat during WAE injection. This results indicates that the timing of WAE designs must be carefully selected.

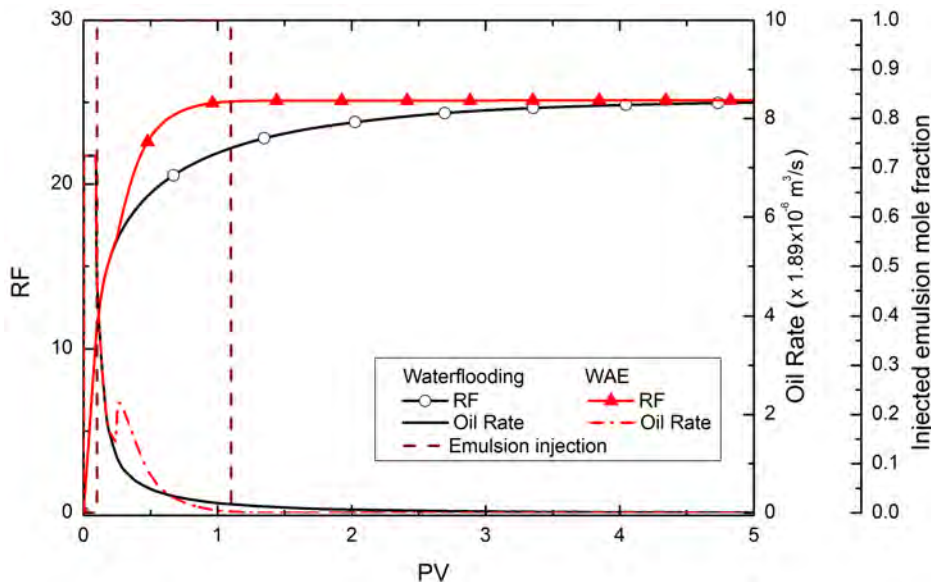


Figure 11. RF for waterflooding and WAE injection using the mobility control mechanism permeability curves presented in Fig.8(b). Emulsion slug was injected at 0.1 PV.

3.3 Case III. Synthetic light-oil relative permeability curves

In this case we generate synthetic relative permeability curves similar to published sets for light-oil in a weakly water-wet media. In the first set of curves, shown in Figure 12(a), the more efficient pore-level displacement of the emulsion flooding was characterized by lowering the residual oil saturation from $S_{orw}=0.40$ to $S_{ore}=0.20$. Although this case presents the lowest viscosity ratio among all cases, our choice of relative permeability curves and viscosity yields a

mobility ratio higher than Case I, but lower than Case II, at $M=6$. As in the previous cases, in a second set displayed in Fig. 12(b), we describe aqueous phase mobility control alone, by fixing the residual oil saturation and lowering the end-point of the emulsion curve with respect to water to yield a mobility ratio of $M=2$. The liquid properties chosen for the simulation were $\mu_o=0.01$ Pa.s, $\rho_o=994.92$ Kg/m³, $\mu_w=0.001$ Pa.s and $\rho_w=997.7$ Kg/m³.

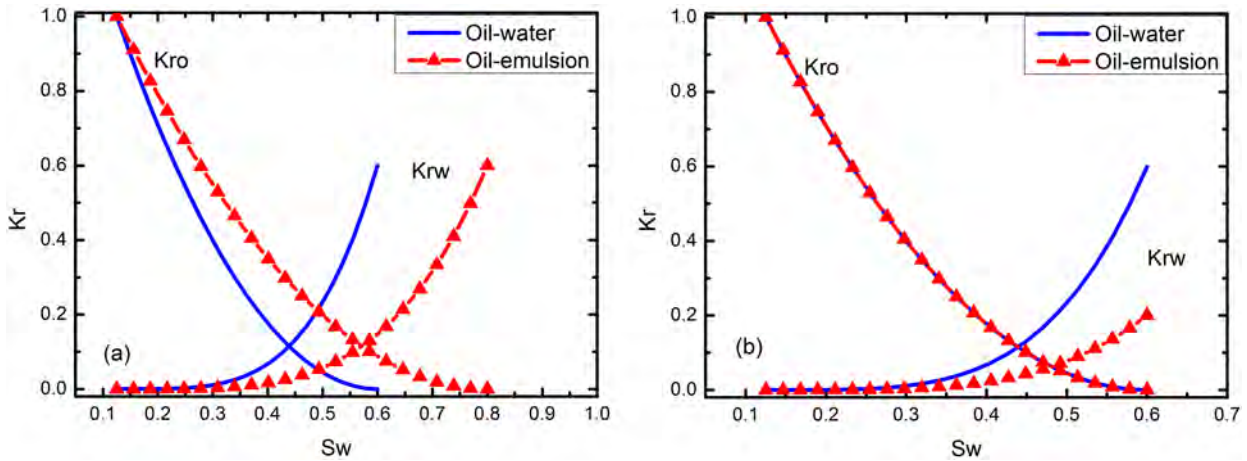


Figure 12. Synthetic Relative permeability curves used in Case III for water and emulsion injection. Fig (a) describes the emulsion pore-level displacement efficiency and Fig. (b) pure mobility control mechanism .

Oil recovery during water and WAE flooding is depicted in Fig. 13. As before, the change in the residual oil saturation during emulsion flooding led to a significant increase in the total volume of oil displaced. In this case, in contrast with the previous two, the mobility control mechanism is able to show a small improvement in oil recovery. This is somewhat unexpected, since the mobility ratio is between those of the other two cases. A possible reason for this is the concavity of the oil relative permeability curve, whose permeability values at intermediate water saturation are much lower than in the other two cases.

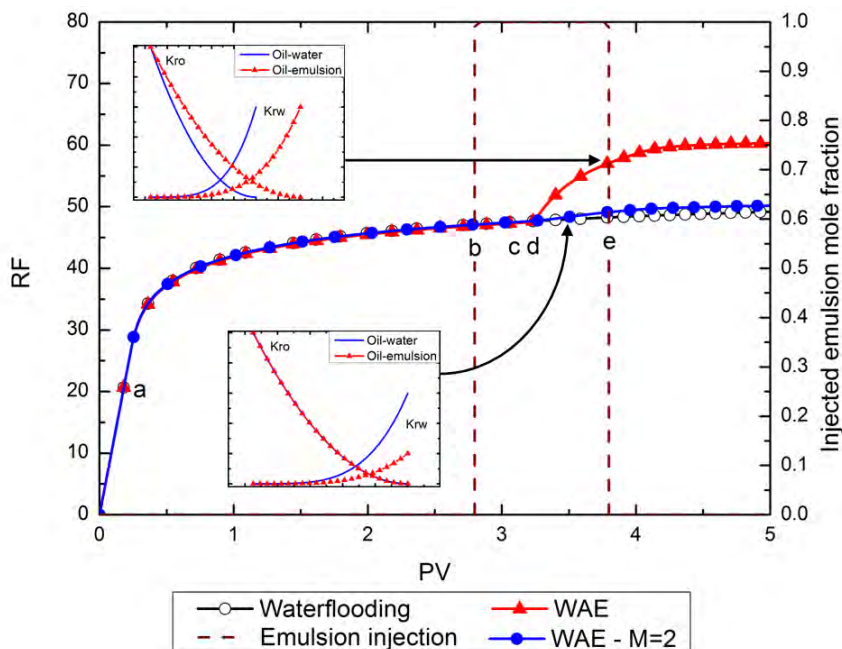


Figure 13. RF for waterflooding and WAE injection using both set of curves presented in Fig. 12. Emulsion slug was injected at 2.8 PV.

The evolution of the water saturation for both emulsion flooding cases are shown in Fig. 14. Because of the oil curve concavity, a sharp variation of the water saturation through the displacement front is observed. Upon injection of pure-mobility control emulsion, the small reduction in oil saturation contributes to oil recovery, in addition to the observed improvement in areal sweep. When WAE injection is carried out after 0.1 PV water slug, a hint of dispersed oil bank is noticed by the acceleration of oil production shown in Fig. 15.

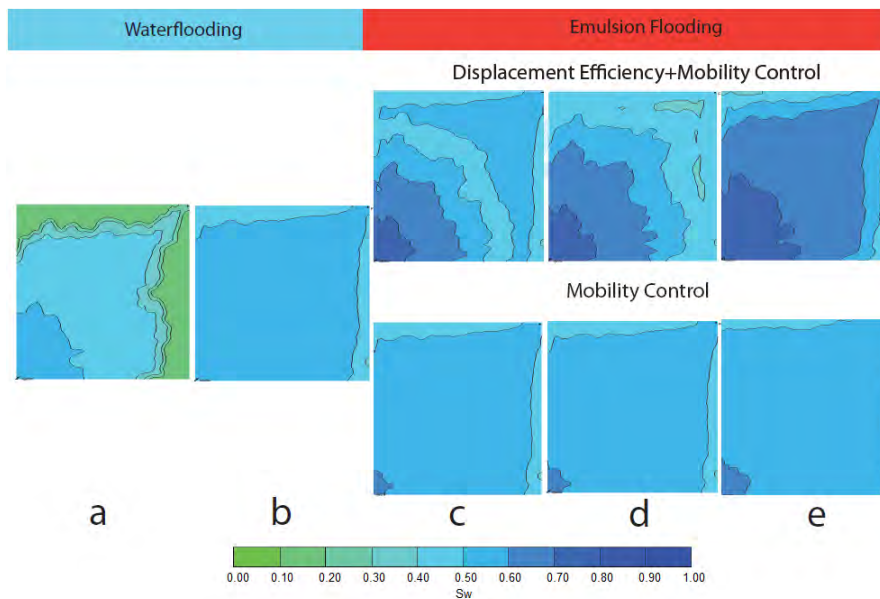


Figure 14. Water saturation maps for WAE injection using the selected times highlighted in Fig. 13 for both sets of relative permeability curves.

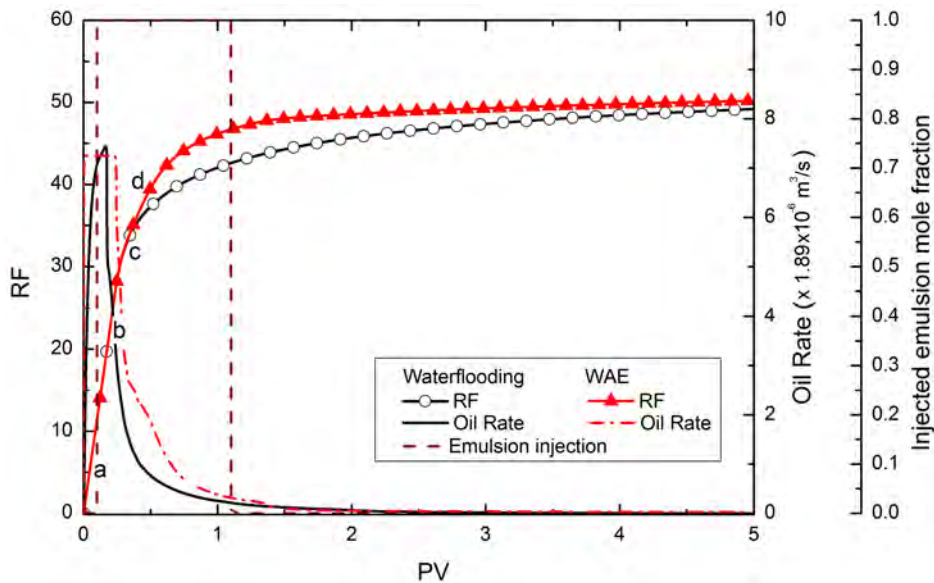


Figure 15. RF for waterflooding and WAE injection using the mobility control mechanism permeability curves presented in Fig.12(b). Emulsion slug was injected at 0.1 PV.

4. CONCLUSIONS

We have successfully modeled displacement efficiency and mobility control mechanisms in emulsion flooding for a broad range of viscosity and mobility ratios using a commercial reservoir simulator. These mechanisms were represented through changes in the relative permeability curves of oil and aqueous phase. The modeling strategy developed allows one to simulate a process we have denominated Water-Alternating-Emulsion (WAE) injection. We exploited this strategy using relative permeability curves from history matching of laboratory production data, from steady-state experiments, and synthetically constructing them. Results show that WAE flooding can be effective even in light oil recovery, at which the mobility ratio is not expected to be unfavorable. In our numerical experiments, for all the cases the production enhancement was associated with the formation of an oil bank ahead of the emulsion displacement front. Regarding to the two mechanism analysed, predictions showed that displacement efficiency has a much stronger impact on ultimate recovery than mobility control alone under WAE processes. However, the timing of emulsion injection has a noticeable impact on the production acceleration, as observed in recovery results for the pure mobility control mechanism. The latter imply that design of emulsion flooding that favors mobilization of residual oil will produce larger benefits. The predictions

suggest that viscosity and mobility ratios alone are insufficient to foresee the flow response of flooding schemes and attention must be paid to details of the relative permeability curves. Further work is desirable to investigate the later evidence as well as the impact of emulsion flooding on vertical sweep efficiency. Additional modeling work is underway to include necessary capillary number effects in pseudo-compositional models of oil-in-water emulsion flooding.

5. ACKNOWLEDGEMENTS

We would like to acknowledge the Brazilian Research Council (CNPq), Petrobras and the Enhanced Oil Recovery Institute (EORI) at the University of Wyoming for financial support.

6. REFERENCES

- Arhuoma, M., Dong, M., Yang, D. and Idem, R., 2009a. "Determination of water-in-oil emulsion viscosity in porous media". *Ind. Eng. Chem. Res.*, Vol. 48, pp. 7092–7102.
- Arhuoma, M., Yang, D., Dong, M., Li, H. and Idem, R., 2009b. "Numerical simulation of displacement mechanisms for enhancing heavy oil recovery during alkaline flooding". *Energy Fuels*, Vol. 23, pp. 5995–6002.
- Cobos, S., Carvalho, M.S. and Alvarado, V., 2009. "Flow of oil-water emulsions through a constricted capillary". *Int. J. Multiphase Flow*, Vol. 35, pp. 507–515.
- Corey, A., 1954. "The interrelation between gas and oil relative permeabilities". *Prod. Mon.*, Vol. 19, pp. 38–41.
- Dong, M., Ma, S. and Liu, Q., 2009. "Enhanced heavy oil recovery through interfacial instability: A study of chemical flooding for brintnell heavy oil". *Fuels*, Vol. 88, pp. 1049–1056.
- Dykstra, H. and Parsons, R.L., 1950. *The prediction of oil recovery by waterflooding in secondary recovery of oil in the united states*. API, New York, 2nd edition.
- Engelke, B., Carvalho, M.S. and Alvarado, V., 2013. "Conceptual darcy-scale model of oil displacement with macroemulsion". *Energy Fuels*, Vol. 27, pp. 1967–1973.
- Guillen, V., Carvalho, M.S. and Alvarado, V., 2012a. "Pore scale and macroscopic displacement mechanism in emulsion flooding". *Transp. Porous Med.*, Vol. 94, pp. 197–206.
- Guillen, V., Romero, M.I., Carvalho, M.S. and Alvarado, V., 2012b. "Capillary-driven mobility control in macro emulsion flow in porous media". *Int. J. Multiphase Flow*, Vol. 43, pp. 62–65.
- Homsy, G.M., 1987. "Viscous fingering in porous media". *Annu. Rev. Fluid Mech.*, Vol. 19, pp. 271–311.
- Jennings, H.Y., Johnson, C.E. and McAuliffe, C.D., 1974. "A caustic waterflooding process for heavy oils". *J. Pet. Technol.*, Vol. 26, pp. 1344–1352.
- Johnson, E.F., Bossler, D.P. and Naumann, V.O., 1959. "Calculation of relative permeability from displacements experiments". *Trans. AIME*, Vol. 216, pp. 370–376.
- Kazempour, M., Sundstrom, E. and Alvarado, V., 2012. "Effect of alkalinity on oil recovery during polymer floods in sandstone". *SPE Reserv. Eval. Eng.*, Vol. 15, pp. 195–209.
- McAuliffe, C.D., 1973a. "Crude-oil-in-water emulsions to improve fluid-flow in an oil reservoir". *J. Pet. Technol.*, Vol. 25, pp. 721–726.
- McAuliffe, C.D., 1973b. "Oil-in-water emulsions and their flow properties in porous media". *J. Pet. Technol.*, Vol. 25, pp. 727–733.
- Payatakes, A.C., 1982. "Dynamics of oil ganglia during immiscible displacement in water-wet porous media". *Ann. Rev. Fluid Mech.*, Vol. 14, pp. 365–393.
- Romero, M.I., Carvalho, M.S. and Alvarado, V., 2011. "Experiments and network model of flow of oil-in-water emulsion in porous media". *Phys. Rev. E*, Vol. 84, p. 046305.
- Sorbie, K.S., 1991. *Polymer improved oil recovery*. CRC Press, Glasgow, Boca Raton, Fla.
- Zhang, H., Dong, M. and Zhao, S., 2010. "Which one is more important in chemical flooding for enhanced court heavy oil recovery, lowering interfacial tension or reducing water mobility?" *Energy Fuels*, Vol. 24, pp. 1829–1836.

7. RESPONSIBILITY NOTICE

The authors are the only responsible for the printed material included in this paper.